Showcasing research from Professor Minami's laboratory, Institute of Industrial Science, The University of Tokyo, Tokyo, Japan.

Spontaneous preparation of a fluorescent ratiometric chemosensor for metal ions using off-the-shelf materials

A self-assembled chemosensor prepared by only mixing off-the-shelf materials shows ratiometric properties upon detecting metal ions. As shown in colored bottles on an array (*i.e.*, the vending machine), the various optical patterns depending on analyte concentrations allowed pattern recognition-driven chemical sensing.

As featured in:

See Tsuyoshi Minami *et al.*, *Chem. Commun.*, 2023, **59**, 7747.

ROYAL SOCIETY OF CHEMISTRY

rsc.li/chemcomm

Registered charity number: 207890

ChemComm

COMMUNICATION

View Article Online
View Journal | View Issue

Cite this: *Chem. Commun.*, 2023, 59, 7747

Received 27th February 2023,
Accepted 11th May 2023

DOI: 10.1039/d3cc00949a

rsc.li/chemcomm

Spontaneous preparation of a fluorescent ratiometric chemosensor for metal ions using off-the-shelf materials†

Yui Sasaki, [a] Kohei Ohshiro, [a] Qi Zhou, [a] Xiaojun Lyu, [a] Wei Tang, [a] Kiyosumi Okabe, [a] Shin-ya Takizawa [b] and Tsuyoshi Minami *[a]

A self-assembled chemosensor prepared using off-the-shelf materials has shown various fluorescence responses including ratiometric and simple ON–OFF switching profiles by adding different toxic metal ions. The unique fingerprint-like responses have been applied to pattern recognition of metal ions in river water for environmental analysis.

Chemosensor arrays using inherent cross-reactivities of artificial receptors[1] are potent analytical tools allowing high-throughput sensing combined with data processing techniques.[2] However, inset data for pattern recognition is conventionally prepared using several chemosensors owing to the limitation of variation of sensor responses, which causes synthetic efforts for the preparation of a chemosensor library.[3] To this end, we herein propose a single self-assembled chemosensor prepared from off-the-shelf materials to discriminate toxic metal ions[4] quantitatively based on pattern recognition for environmental assessment.

In contrast to typical indicator–spacer–receptor-based chemosensors that are covalently connected,[5] indicator displacement assay (IDA)-based chemosensors are easily obtained by non-covalent bonds between indicators and receptors.[6] However, the conventional IDA-based fluorescent chemosensors show only simple switching profiles such as ON–OFF (or OFF–ON) responses because indicators do not contribute to analyte capture.[7] In the case of ON–OFF or OFF–ON-type chemosensors, the discrimination of a response for analyte detection from background noise in the real-sample analysis is a concern because of the single fluorescence channel.[8] On the other hand, ratiometric responses possessing two-fluorescence color channels can reduce false-positive signals originating from interference effects.[4b,9] Thus, ratiometric-type chemosensors are promising materials for real-sample analysis;[8b,10] however multi-step organic synthesis is generally required to obtain a fluorescent ratiometric chemosensor.[11] Hence, we decided to design a ratiometric self-assembled chemosensor based on a catechol dye that acts as not only an indicator but also a binding unit to increase optical response patterns in a competitive assay.[12]

A coumarin derivative (*i.e.*, esculetin (EL)) as an off-the-shelf catechol fluorophore is capable of interacting with not only target metal ions through a coordination bond[13] but also a phenylboronic acid (PBA) derivative through a dynamic covalent bond.[7,11a] The coordination of EL and a metal ion offers fluorescence changes, whereas the spectral shifts of EL upon adding metal ions are not significant. Namely, the fluorescence changes in one channel are dominant. In this assay, a self-assembled complex of EL and 3-nitrophenylboronic acid (3-NPBA) was employed as a fluorescent chemosensor for metal ions (Fig. 1). A fluorescence change in EL occurs upon the formation of the boronate/boronic ester,[14] owing to photoinduced electron transfer (PeT) from the excited state of EL to the nitrophenyl moiety of 3-NPBA.[7b,15] In our strategy, the absolute fluorescence intensity of EL is purposely manipulated by 3-NPBA. Therefore, the fluorescence responses of EL in the presence of 3-NPBA upon adding analyte metal ions can be

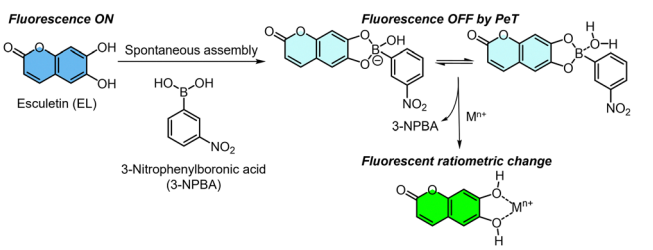

Fig. 1 Schematic of the fluorescence detection mechanism of the self-assembled chemosensor, comprising esculetin (EL) and 3-nitrophenylboronic acid (3-NPBA), for metal ions.

[a] *Institute of Industrial Science, The University of Tokyo, 4-6-1 Komaba, Meguro-ku, Tokyo, 153-8505, Japan. E-mail: tminami@g.ecc.u-tokyo.ac.jp*
[b] *Department of Basic Science, Graduate School of Arts and Sciences, The University of Tokyo, 3-8-1, Komaba, Meguro-ku, Tokyo, 153-8902, Japan*

† Electronic supplementary information (ESI) available: Selected UV-vis and fluorescence titration results, photophysical properties, discussion of binding stoichiometry, and array experiments. See DOI: https://doi.org/10.1039/d3cc00949a

apparently observed as significant changes. The approach provides various optical responses including ratiometric and simple ON–OFF switching profiles with the difference in target metal ions, which contributes to pattern recognition-driven chemical sensing.

The optical properties in this competitive assay were evaluated step-by-step. In the UV-vis titration of 3-NPBA, a nonlinear saturation curve obtained from stepwise blueshifts of UV-vis absorption spectra of EL indicated the formation of the boronate ester of the catechol chromophore and 3-NPBA (Fig. S1, ESI†). In addition, the fluorescence intensity of EL decreased upon the addition of 3-NPBA (Fig. S2, ESI†), owing to PeT.[6,7b] In this regard, emission quantum yields (φ) of EL and the EL–3-NPBA complex were determined to be 21% and 3%, respectively (Table S1, ESI†). Meanwhile, almost no change in the lifetime (τ) of EL before and after adding 3-NPBA was observed (Table S1, ESI†), implying a static quenching mechanism.[16] The complexation between EL and 3-NPBA with a 1 : 1 stoichiometry was also supported by electrospray ionization-mass spectrometry (ESI-MS) analysis.[7b] Judging from the complexation rate of 99% in the fluorescence titration (Fig. S2, ESI†), the molar ratio of EL and 3-NPBA for the further demonstration of detecting metal ions was decided as 1 : 60.

Next, the optical response changes of the EL–3-NPBA complex upon adding metal ions were assessed. The fluorescence spectra of the EL–3-NPBA complex were red-shifted upon the addition of a metal ion (*i.e.*, Pb^{2+}) (Fig. 2(a), left). Indeed, the change in the fluorescence color was recognized by the naked eye, showing a ratiometric behavior. Certainly, the fluorescence response at 543 nm of the EL–3-NPBA complex with an increase in Pb^{2+} concentration was significant in comparison to that in the absence of 3-NPBA, which indicated the contribution of 3-NPBA to the ratiometric fluorescence changes (Fig. S28, ESI†). The lifetime measurements of EL in the presence of Pb^{2+} presented two components (τ_1 and τ_2), which could be attributed to the EL–Pb^{2+} complex and EL, respectively. In this regard, the lifetime of EL was not influenced even in the presence of 3-NPBA (Table S1, ESI†). Moreover, Fig. 2(b) shows the quantitative ratiometric fluorescence changes upon adding Zn^{2+}. The ESI-MS analysis results supported the complexation of EL and Zn^{2+} with a 1 : 1 stoichiometry (Fig. 2(b), right). In accordance with the 1 : 1 binding mode, the apparent binding constant of EL to Zn^{2+} in the presence of 3-NPBA was estimated to be $(8.3 \pm 0.4) \times 10^2\ M^{-1}$. Although the EL–$Pb^{2+}$ complex with a 1 : 1 stoichiometry in the presence of 3-NPBA was observed in ESI-MS analysis (Fig. 2(a), right), a nonlinear curve fitting based on a 1 : 1 binding stoichiometry was not achieved owing to the biphasic behavior[17] (for more details, see the ESI†). Subsequently, a selectivity test of the self-assembled chemosensor for 13 metal ions (*i.e.*, Pb^{2+}, Zn^{2+}, Cu^{2+}, Ni^{2+}, Hg^{2+}, Cd^{2+}, Co^{2+}, Ca^{2+}, K^+, Na^+, Mg^{2+}, Ba^{2+}, and Cs^+) was carried out. Other metal ions including Al^{3+}, Sn^{2+}, Fe^{2+}, Cr^{3+}, and Ga^{3+} were excluded from the metal ion library because of hydrolysis under the measurement conditions. The EL–3-NPBA complex did not respond to Ca^{2+}, K^+, Na^+, Mg^{2+}, Ba^{2+}, and Cs^{2+} owing to their low binding affinities to a coumarin derivative (Fig. S22–S27, ESI†).[13a] Although the UV-vis absorption spectra of the EL–3-NPBA complex changed upon the addition of Hg^{2+} and Cd^{2+} at high concentrations (Fig. S7 and S8, ESI†), significant spectral changes were not observed in fluorescence titrations. The EL–3-NPBA complex exhibited different ON–OFF responses upon addition of Pb^{2+}, Zn^{2+}, Ni^{2+}, Co^{2+}, and Cu^{2+} (Fig. 3(a)), and the magnitudes of the determinable apparent binding constants were approximately 10^2 to $10^3\ M^{-1}$. Among them, the EL–3-NPBA complex showed ratiometric fluorescence responses to Pb^{2+} and Zn^{2+} (Fig. 3(b)). Notably, the response of EL to Cu^{2+} was significant compared to Pb^{2+} at λ_{em} = 472 nm (Fig. 3(a)), although a ratiometric behavior to Cu^{2+} was not observed (Fig. 3(b)). In addition, the responses to Ni^{2+} and Co^{2+} at high concentrations were also non-ratiometric ON–OFF switching profiles. Therefore, the obtained concentration-dependent fluorescence response pattern including ratiometric and simple ON–OFF switching profiles indicated its potential for pattern recognition. As an additional evaluation, NMR analysis was also carried out to investigate the complexation of EL and Pb^{2+} in the presence of 3-NPBA; however evidence to support the complexation of EL and Pb^{2+} in the presence of 3-NPBA was not provided by NMR analysis.[18]

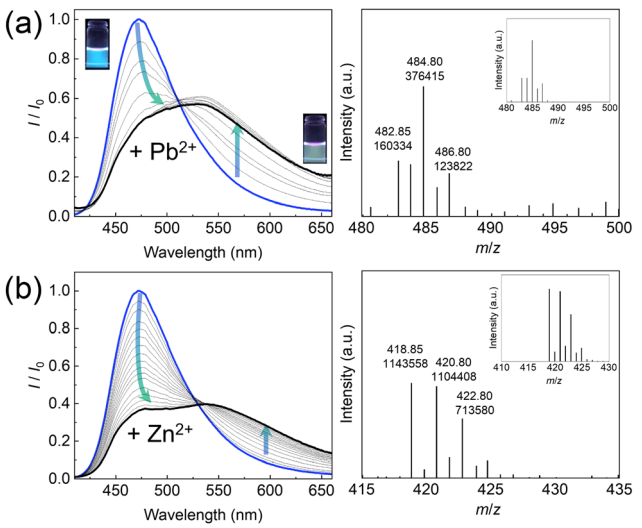

Fig. 2 (Left) Changes in fluorescence spectra of EL (4 μM) with 3-NPBA (240 μM) upon adding (a) Pb^{2+} (0–70 μM) and (b) Zn^{2+} (0–2000 μM) in a HEPES buffer (50 mM) at pH 7.4 at 25 °C. λ_{ex} = 388 nm. (Right) ESI-MS spectra for (a) the EL–Pb^{2+} complex and (b) the EL–Zn^{2+} complex. Insets indicate calculated isotope patterns. MS (ESI, +) *m*/*z*: $[EL + Pb + ClO_4]^+$, calcd for $C_9H_6ClO_8Pb$ 484.95; found: 484.80. $[EL + Zn + ClO_4 + DMSO]^+$, calcd for $C_{11}H_{12}ClO_9SZn$ 418.92; found: 418.85. [EL] = [3-NPBA] = 1 mM, $[Pb^{2+}] = [Zn^{2+}]$ = 2 mM. Solvent/eluent: methanol.

As the next attempt, the chemosensor was applied to pattern recognition (*e.g.*, a semi-quantitative assay) of Cu^{2+}, Pb^{2+}, and Zn^{2+} which could act as inhibitors to root growth.[19] The semi-quantitative assay was not performed for Ni^{2+} and Co^{2+} because a situation requiring the detection of these metal ions at high concentrations (mM levels) is not realistic in practical sensing. In this assay, the inset data for pattern recognition was constructed from the fluorescence changes of the EL–3-NPBA

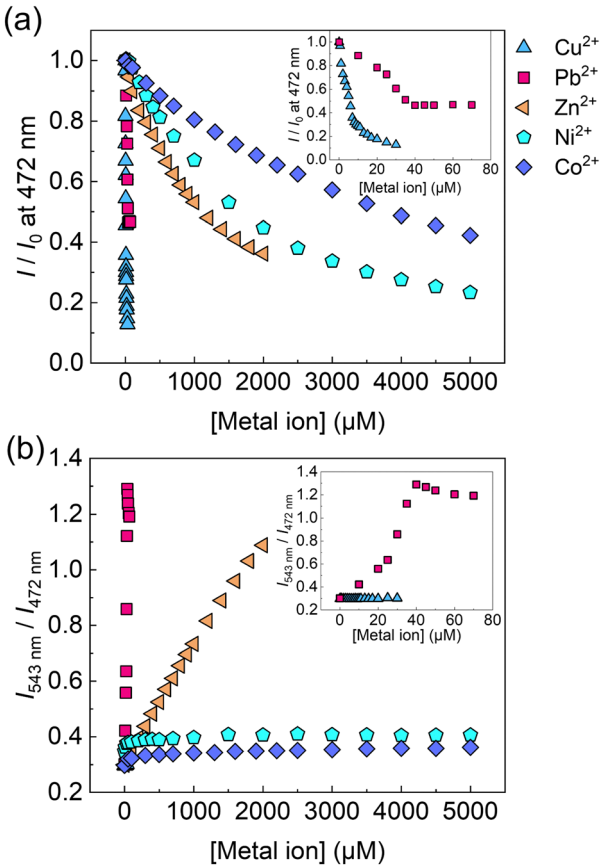

Fig. 3 Fluorescence changes in EL (4 μM) with 3-NPBA (240 μM) upon adding metal ions (*i.e.*, Pb^{2+}, Zn^{2+}, Cu^{2+}, Ni^{2+}, and Co^{2+}) in a HEPES buffer (50 mM) at pH 7.4 at 25 °C. λ_{ex} = 388 nm. (a) Titration isotherm for the metal ions obtained by plotting the maximum emission at 472 nm. (b) Emission ratio ($I_{543\ nm}/I_{472\ nm}$) of EL–3-NPBA upon adding the metal ions. Each inset indicates the fluorescence changes at low concentration ranges.

complex upon the addition of Cu^{2+}, Pb^{2+}, or Zn^{2+} at different concentrations. The data matrix obtained from the fluorescence measurements was treated using the Student's *t*-test to exclude outliers of 4 repetitive data points from 24 repetitive data points. The treated dataset contains multi-dimensional information that was constructed by 1 chemosensor × 3 analytes (Cu^{2+}, Pb^{2+}, and Zn^{2+}) × 5 concentrations ([Cu^{2+}] = 0–1.3 ppm, [Pb^{2+}] = 0–8.3 ppm, and [Zn^{2+}] = 0–65 ppm) × 58 wavelength points (ranging from 415 to 700 nm, in 5 nm interval of λ_{em}) × 20 repetitions, obtaining 17 400 data points in total. The inset data was subsequently treated using linear discriminant analysis (LDA), which is capable of classification of clusters and decreasing the multi-dimensional information. Through the data processing with LDA, the multi-dimensional inset data can be visualized as two- (Factor 1 (F1), F2) or three-dimensional (F1, F2, and F3) canonical score plots. The values of each factor represent a contribution of the inputted data matrix for the discrimination.[2a] Fig. 4 shows a concentration-dependent distribution of each cluster with a 100% correct classification. Each cluster of Zn^{2+} and Pb^{2+} containing 20 repetitive datasets was nonlinearly distributed in accordance

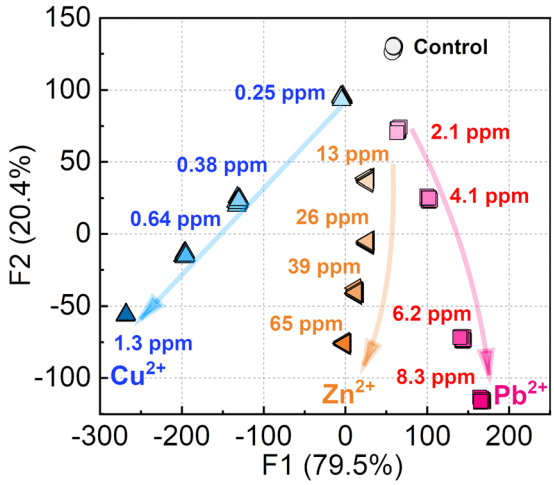

Fig. 4 Semi-quantitative assay for Pb^{2+}, Zn^{2+}, and Cu^{2+} using the single self-assembled chemosensor. The ability of the chemosensor to discriminate was revealed by LDA with a classification rate of 100%. 20 repetitive measurements were carried out for each concentration.

with the increase in the concentrations, originating from the ratiometric responses. On the other hand, the positions of clusters of Cu^{2+} indicated linearity stemmed from a simple ON–OFF response.

Finally, the single chemosensor was applied to a real-sample analysis with river water. To evaluate the applicability of the chemosensor to environmental assessment, a support vector machine (SVM)[20] was employed. The calibration line was built using the inset data constructed from seven different concentrations of Pb^{2+} (gray circles), followed by the prediction of two concentrations of unknown samples (pink squares). In Fig. 5, the predicted clusters at 3.1 and 7.3 ppm were distributed on the calibration line with a low root mean square error for the prediction (RMSEP) value. Taken together, the accurate prediction of unknown concentrations of the target metal ion in river

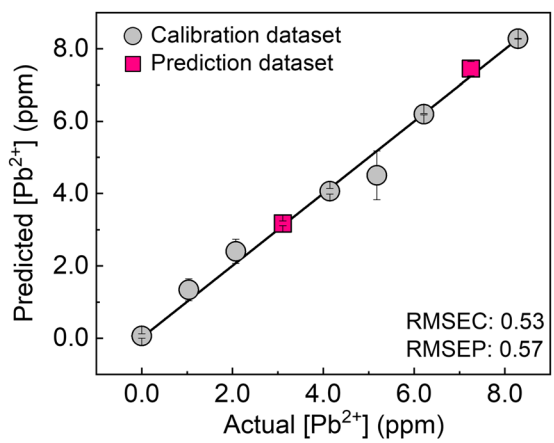

Fig. 5 Quantitative assay against Pb^{2+} in river water by using SVM. Root mean square errors for calibration (RMSEC) and prediction (RMSEP) represent the quality of the built model and prediction. 20 repetitive measurements were carried out for each concentration.

water was achieved by the ratiometric responses based on molecular self-assembly.

In summary, we designed a single self-assembled fluorescent ratiometric chemosensor for the simultaneous discrimination of metal ions using off-the-shelf materials. A catechol fluorophore EL spontaneously interacted with 3-NPBA, which caused fluorescence quenching by PeT. Notably, the self-assembled chemosensor displayed ratiometric responses upon the addition of Pb^{2+} and Zn^{2+}, indicating the feasibility of pattern recognition using a single chemosensor. Indeed, the single self-assembled chemosensor achieved a semi-quantitative assay of Pb^{2+}, Zn^{2+}, and Cu^{2+} with high accuracy. Furthermore, a regression analysis of Pb^{2+} in river water was demonstrated using a machine learning method, and the favorable applicability to real-sample analysis was revealed by the accurate prediction of unknown concentrations of Pb^{2+} in river water. Further investigation to understand the unique optical properties of the self-assembled chemosensing system is required, while we believe that our approach to maximizing the power of molecular self-assemblies could be used for not only metal ion detections but also for other species because of the abundant combination of building blocks.

T. Minami thanks the financial support from the Japan Society for the Promotion of Science (JSPS KAKENHI Grant No. JP23H03864 and JP21H01780) and JST CREST (Grant No. JPMJCR2011). Y. Sasaki also thanks the special fund of Institute of Industrial Science, the University of Tokyo, the JSPS KAKENHI (Grant No. JP22K14706). K. Ohshiro, Q. Zhou, and X. Lyu thank the JSPS Research Fellow for Young Scientists (DC1) (Grant No. JP23KJ0785, JP22J23433, and JP22J23435, respectively).

Conflicts of interest

There are no conflicts of interest to declare.

References

1 (*a*) T. A. Dickinson, J. White, J. S. Kauer and D. R. Walt, *Nature*, 1996, **382**, 697–700; (*b*) K. J. Albert, N. S. Lewis, C. L. Schauer, G. A. Sotzing, S. E. Stitzel, T. P. Vaid and D. R. Walt, *Chem. Rev.*, 2000, **100**, 2595–2626.

2 (*a*) P. Anzenbacher Jr, P. Lubal, P. Buček, M. A. Palacios and M. E. Kozelkova, *Chem. Soc. Rev.*, 2010, **39**, 3954–3979; (*b*) Z. Li, J. R. Askim and K. S. Suslick, *Chem. Rev.*, 2019, **119**, 231–292; (*c*) Y. Geng, W. J. Peveler and V. M. Rotello, *Angew. Chem., Int. Ed.*, 2019, **58**, 5190–5200; (*d*) Y. Sasaki, R. Kubota and T. Minami, *Coord. Chem. Rev.*, 2021, **429**, 213607.

3 (*a*) Y. Sasaki, S. Kojima, V. Hamedpour, R. Kubota, S. Takizawa, I. Yoshikawa, H. Houjou, Y. Kubo and T. Minami, *Chem. Sci.*, 2020, **11**, 3790–3796; (*b*) Y. Liu, T. Minami, R. Nishiyabu, Z. Wang and P. Anzenbacher Jr, *J. Am. Chem. Soc.*, 2013, **135**, 7705–7712.

4 (*a*) S. Bolisetty, M. Peydayesh and R. Mezzenga, *Chem. Soc. Rev.*, 2019, **48**, 463–487; (*b*) H. Jin, M. Yang, Z. Sun and R. Gui, *Coord. Chem. Rev.*, 2021, **446**, 214114.

5 For reviews, see: (*a*) D. Wu, A. C. Sedgwick, T. Gunnlaugsson, E. U. Akkaya, J. Yoon and T. D. James, *Chem. Soc. Rev.*, 2017, **46**, 7105–7123; (*b*) Y. Fang and W. Dehaen, *Coord. Chem. Rev.*, 2021, **427**, 213524; for examples, see: (*c*) K. Rout, A. K. Manna, M. Sahu, J. Mondal, S. K. Singh and G. K. Patra, *RSC Adv.*, 2019, **9**, 25919–25931; (*d*) C. A. S. Pothulapadu, A. Jayaraj, N. Swathi, R. N. Priyanka and G. Sivaraman, *ACS Omega*, 2021, **6**, 24473–24483.

6 (*a*) B. T. Nguyen and E. V. Anslyn, *Coord. Chem. Rev.*, 2006, **250**, 3118–3127; (*b*) A. C. Sedgwick, J. T. Brewster, T. Wu, X. Feng, S. D. Bull, X. Qian, J. L. Sessler, T. D. James, E. V. Anslyn and X. Sun, *Chem. Soc. Rev.*, 2021, **50**, 9–38.

7 (*a*) X. Liang and M. Bonizzoni, *J. Mater. Chem. B*, 2016, **4**, 3094–3103; (*b*) Y. Sasaki, É. Leclerc, V. Hamedpour, R. Kubota, S. Takizawa, Y. Sakai and T. Minami, *Anal. Chem.*, 2019, **91**, 15570–15576.

8 (*a*) L. Gao, W. Wang, X. Wang, F. Yang, L. Xie, J. Shen, M. A. Brimble, Q. Xiao and S. Q. Yao, *Chem. Soc. Rev.*, 2021, **50**, 1219–1250; (*b*) Y. Zheng, Y. Ding, X. Zheng, C. Zhang, Y. Zhang, Y. Xiang and A. Tong, *Anal. Chem.*, 2021, **93**, 10272–10281.

9 (*a*) M. H. Lee, J. S. Kim and J. L. Sessler, *Chem. Soc. Rev.*, 2015, **44**, 4185–4191; (*b*) S.-H. Park, N. Kwon, J.-H. Lee, J. Yoon and I. Shin, *Chem. Soc. Rev.*, 2020, **49**, 143–179.

10 (*a*) Y. Han, C. Ding, J. Zhou and Y. Tian, *Anal. Chem.*, 2015, **87**, 5333–5339; (*b*) Z. Liu, X. Jing, S. Zhang and Y. Tian, *Anal. Chem.*, 2019, **91**, 2488–2497.

11 (*a*) K. Sakakibara, L. A. Joyce, T. Mori, T. Fujisawa, S. H. Shabbir, J. P. Hill, E. V. Anslyn and K. Ariga, *Angew. Chem., Int. Ed.*, 2012, **51**, 9643–9646; (*b*) A. Kaur, H. Sharma, S. Kaur, N. Singh and N. Kaur, *RSC Adv.*, 2013, **3**, 6160–6166; (*c*) L. Tang, D. Wu, X. Wen, X. Dai and K. Zhong, *Tetrahedron*, 2014, **70**, 9118–9124; (*d*) J. Y. Lee, H. D. Root, R. Ali, W. An, V. M. Lynch, S. Bähring, I. S. Kim, J. L. Sessler and J. S. Park, *J. Am. Chem. Soc.*, 2020, **142**, 19579–19587; (*e*) N. Dey, B. Maji and S. Bhattacharya, *Chem. – Asian J.*, 2018, **13**, 664–671.

12 (*a*) Y. Kubo, T. Ishida, A. Kobayashi and T. D. James, *J. Mater. Chem.*, 2005, **15**, 2889–2895; (*b*) T. Minami, F. Emami, R. Nishiyabu, Y. Kubo and P. Anzenbacher Jr, *Chem. Commun.*, 2016, **52**, 7838–7841; (*c*) Y. Sasaki, T. Minamiki, S. Tokito and T. Minami, *Chem. Commun.*, 2017, **53**, 6561–6564.

13 (*a*) L. Zhang, S. Dong and L. Zhu, *Chem. Commun.*, 2007, 1891–1893; (*b*) Y. Sasaki, X. Lyu, R. Kubota, S. Takizawa and T. Minami, *ACS Appl. Bio Mater.*, 2021, **4**, 2113–2119.

14 (*a*) S. D. Bull, M. G. Davidson, J. M. H. van den Elsen, J. S. Fossey, A. T. A. Jenkins, Y.-B. Jiang, Y. Kubo, F. Marken, K. Sakurai, J. Zhao and T. D. James, *Acc. Chem. Res.*, 2013, **46**, 312–326; (*b*) S. Cho, S. Y. Hwang, D. X. Oh and J. Park, *J. Mater. Chem. A*, 2021, **9**, 14630–14655.

15 (*a*) B. Daly, J. Ling and A. P. de Silva, *Chem. Soc. Rev.*, 2015, **44**, 4203–4211; (*b*) T. Ueno, Y. Urano, H. Kojima and T. Nagano, *J. Am. Chem. Soc.*, 2006, **128**, 10640–10641.

16 L. K. Fraiji, D. M. Hayes and T. C. Werner, *J. Chem. Educ.*, 1992, **69**, 424.

17 (*a*) S. C. McCleskey, A. Metzger, C. S. Simmons and E. V. Anslyn, *Tetrahedron*, 2002, **58**, 621–628; (*b*) A. Le Person, A. Moncomble and J.-P. Cornard, *J. Phys. Chem. A*, 2014, **118**, 2646–2655.

18 NMR analysis was carried out to investigate the complexation of EL and Pb^{2+} in the presence of 3-NPBA; however a precipitate was obtained under the high concentration conditions of the components (>500 μM) in D_2O at pD 7.4. The coordination between the hydroxyl groups of EL and Pb^{2+} caused a dramatic decrease in the solubility of EL in the aqueous solution, and consequently a solid-state product originating from the EL–Pb^{2+} complex was unexpectedly precipitated. Overall, evidence to support the complexation of EL and Pb^{2+} was not provided by NMR analysis because the sensitivity of the saturated solution mixture was not satisfactory for the NMR measurements.

19 S. M. Palacio, F. R. Espinoza-Quiñones, R. M. Galante, D. C. Zenatti, A. A. Seolatto, E. K. Lorenz, C. E. Zacarkim, N. Rossi, M. D. A. Rizzutto and M. H. Tabacniks, *Braz. Arch. Biol. Technol.*, 2005, **48**, 191–196.

20 L. Hamel, *Knowledge Discovery with Support Vector Machines*, Wiley, New Jersey, 2009.

